COMPUTER METHODS IN APPLIED MECHANICS AND ENGINEERING 59 (1986) 307–325
NORTH-HOLLAND

DISCONTINUITY-CAPTURING FINITE ELEMENT FORMULATIONS FOR NONLINEAR CONVECTION-DIFFUSION-REACTION EQUATIONS*

T.E. TEZDUYAR
Department of Mechanical Engineering, University of Houston, Houston, TX 77004, U.S.A.

Y.J. PARK
Department of Chemical Engineering, University of Houston, Houston, TX 77004, U.S.A.

Received 14 March 1986
Revised manuscript received 8 May 1986

Formulations which complement the streamline-upwind/Petrov–Galerkin procedure are presented. These formulations minimize the oscillations about sharp internal and boundary layers in convection-dominated and reaction-dominated flows. The proposed methods are tested on various single- and multi-component transport problems.

1. Introduction

In this paper we investigate new stable and accurate finite element techniques for steady-state coupled nonlinear convection-diffusion-reaction equation systems. Our intent is to contribute to the computational analysis of electrophoresis separation phenomena as well as of chemical reactor design and process control. Prediction of temperature and concentration fields is of critical importance for the safe and economical operation of biochemical and chemical engineering processes.

The set of equations governing the chemically reacting systems include coupling terms in the form of Arrhenius kinetics expression. This expression involves the concentrations and an exponential function of the temperature. Deans and Lapidus [2, 3] and several other authors [4–6, 12–14] have modelled, numerically analyzed, and performed experiments on reactor behaviors. They observed the steady-state multiplicity and the oscillatory behavior of the continuous flow reactors. However, these models and numerical analyses are based on the plug flow (i.e., uniform velocity profile) assumption. In real applications the flow velocity may vary from one point to another both in magnitude and direction. Because of this, the governing equations may vary in nature from convection-dominated to reaction-dominated. In both extreme cases numerical treatment of the problem becomes a significant challenge.

For convection-dominated problems, especially in the presence of discontinuities,

*This research was sponsored by NASA under contract NAS-9-17380 and by NSF under grant NSF MEA-8404810. We are grateful for the computing resources made available by the Aerosciences Branch of the NASA Johnson Space Center. Y.J. Park was sponsored by the Laboratory for Enhanced Oil Recovery, University of Houston.

(Bubnov–) Galerkin formulations may result in spurious oscillations causing in turn a severe loss of accuracy and stability. Some Petrov–Galerkin formulations, such as the streamline-upwind/Petrov–Galerkin (SUPG) formulation of Hughes and Brooks [7] and the sigma weighting and transport weighting methods of Hughes et al. [8], produce to a great extent accurate and oscillation-free solutions. However, these formulations do not preclude overshooting and undershooting along discontinuities. A recent "discontinuity-capturing term" approach by Hughes et al. [9, 10] seems to result in a significantly better behavior along such discontinuities.

Our Petrov–Galerkin formulation, similar to the schemes mentioned above, involves weighting functions constructed by adding two perturbation terms to the functions which would otherwise lead to a Galerkin formulation. The term which acts in the direction of the convection is essentially a SUPG term and depends on the spatial discretization. The second term, which acts in the direction of the gradient in the solution (temperature, concentrations, etc.), depends on the spatial discretization and the magnitude of the "jump" in the solution across an element in the direction of the gradient. It also depends on the cosine of the angle between the velocity and the gradient vectors; this dependence is represented by a continuous function which vanishes at the end points of its domain.

For reaction-dominated problems in the presence of sharp gradients due to high reaction rates, one may again encounter spurious oscillations. This might happen as the velocity at a point assumes or approaches the value zero. Our one-dimensional analysis shows that, by adding a second-order term (with a coefficient depending on a dimensionless number constructed from the reaction rate, convection speed, and the element length) to the differential equation, one can minimize such oscillations. From this analysis one can determine the coefficient of this second-order term, which leads to nodally exact solutions for one-dimensional linear problems. It is important to note that the contribution of this second-order term becomes significant only where the reaction rate is very high; the preservation of accuracy elsewhere in the domain where the reaction rate is not as high is thus assured.

In Section 2 we introduce the differential equations and the boundary conditions for the convection diffusion-reaction systems. The finite element discretization and the formulations for the convection-dominated flows are given in Section 3. Section 4 describes the procedures for the reaction-dominated problems. The numerical examples and the conclusions are presented in Sections 5 and 6.

2. Problem statement

Consider an n_{sd}-space dimensional homogenous or pseudohomogeneous domain Ω, where convection, diffusion, and chemical reaction of several species occur. Since all chemical reactions involve some level of heat of reaction, we need to track the temperature field in this domain. We assume that the density is constant for the temperature range in the domain and the bulk flow field is either given in closed form or has previously been determined by computational methods. Therefore, the unknowns in this problem are the concentrations of the species and the temperature. We will consider two species with, for simplicity, only a first-order irreversible reaction $A \rightarrow bB$, where A is the reactant, B is the product, and b is the stoichiometric coefficient of the reaction.

The governing equations are based on the total heat and the species material balance. For the steady-state cases they are given as follows:

$$\boldsymbol{u}\cdot\nabla T-\nabla\cdot(\boldsymbol{\kappa}^{T}\cdot\nabla T)-(\Delta H/(\rho c_p))k_0 C^{A}\exp(-E/(RT))=0\,, \tag{2.1}$$

$$\boldsymbol{u}\cdot\nabla C^{A}-\nabla\cdot(\boldsymbol{\kappa}^{A}\cdot\nabla C^{A})+k_0 C^{A}\exp(-E/(RT))=0\,, \tag{2.2}$$

$$\boldsymbol{u}\cdot\nabla C^{B}-\nabla\cdot(\boldsymbol{\kappa}^{B}\cdot\nabla C^{B})-bk_0 C^{A}\exp(-E/(RT))=0\,. \tag{2.3}$$

Here $T=T(\boldsymbol{x})$ is the temperature, while $C^{A}(\boldsymbol{x})$ and $C^{B}(\boldsymbol{x})$ are the concentrations of the reactant and the product for $\boldsymbol{x}\in\Omega\subset\mathbb{R}^{n_{\mathrm{sd}}}$. The velocity field is represented by $\boldsymbol{u}=\boldsymbol{u}(\boldsymbol{x})$ and the diffusivity tensors for the temperature, reactant, and the product are denoted by $\boldsymbol{\kappa}^{T}=\boldsymbol{\kappa}^{T}(\boldsymbol{x})$, $\boldsymbol{\kappa}^{A}=\boldsymbol{\kappa}^{A}(\boldsymbol{x})$, and $\boldsymbol{\kappa}^{B}=\boldsymbol{\kappa}^{B}(\boldsymbol{x})$, respectively. The chemical reaction term, expressed by the Arrhenius kinetics, is $k_0\exp(-E/(RT))$, where k_0 is the reaction rate coefficient, E is the activation energy, and R is the gas constant. The term ρc_p is the heat capacity per unit volume and ΔH is the heat of reaction per mole of the reactant. The equations (2.1)–(2.3) can be rewritten in the following form:

$$\boldsymbol{u}\cdot\nabla\phi^{i}-\nabla\cdot(\boldsymbol{\kappa}^{i}\cdot\nabla\phi^{i})+B^{i}\phi^{2}=0\,,\quad i=1,\ldots,n_{\mathrm{dof}}\,, \tag{2.4}$$

where

$$\boldsymbol{\phi}=\begin{pmatrix}\phi^{1}\\ \phi^{2}\\ \phi^{3}\end{pmatrix}=\begin{pmatrix}T\\ C^{A}\\ C^{B}\end{pmatrix}, \tag{2.5}$$

$$\boldsymbol{B}=\begin{pmatrix}B^{1}\\ B^{2}\\ B^{3}\end{pmatrix}=\begin{pmatrix}(\Delta H/(\rho c_p))k_0\exp(-E/(R\phi^{1}))\\ k_0\exp(-E/(R\phi^{1}))\\ -bk_0\exp(-E/(R\phi^{1}))\end{pmatrix}, \tag{2.6}$$

$$\boldsymbol{\kappa}=\begin{pmatrix}\boldsymbol{\kappa}^{1}\\ \boldsymbol{\kappa}^{2}\\ \boldsymbol{\kappa}^{3}\end{pmatrix}=\begin{pmatrix}\boldsymbol{\kappa}^{T}\\ \boldsymbol{\kappa}^{A}\\ \boldsymbol{\kappa}^{B}\end{pmatrix}, \tag{2.7}$$

and n_{dof} is the number of degrees of freedom.

The boundary Γ of the domain Ω is assumed to be decomposed as follows:

$$\Gamma=\overline{\Gamma_{g^i}\cup\Gamma_{h^i}}\,, \tag{2.8}$$

$$\emptyset=\Gamma_{g^i}\cap\Gamma_{h^i}\,. \tag{2.9}$$

The boundary is allowed to have both Dirichlet- and Neumann-type conditions given below, respectively:

$$\phi^{i}(\boldsymbol{x})=g^{i}(\boldsymbol{x})\quad\forall\boldsymbol{x}\in\Gamma_{g^i}\,,\ i=1,\ldots,n_{\mathrm{dof}}\,, \tag{2.10}$$

$$\boldsymbol{n}(\boldsymbol{x})\cdot\boldsymbol{\kappa}^{i}(\boldsymbol{x})\cdot\nabla\phi^{i}(\boldsymbol{x})=h^{i}(\boldsymbol{x})\quad\forall\boldsymbol{x}\in\Gamma_{h^i}\,,\ i=1,\ldots,n_{\mathrm{dof}}\,, \tag{2.11}$$

where $\boldsymbol{n}$ is the unit outward normal vector to the boundary while g^i and h^i are prescribed functions. Our objective is to determine the unknown vector variable $\boldsymbol{\phi} = \boldsymbol{\phi}(\boldsymbol{x})$ on $\bar{\Omega}$ which satisfies (2.4), (2.10), and (2.11).

3. Finite element formulation

Consider a discretization of Ω into element subdomains Ω^e, $e = 1, 2, \ldots, n_{\text{el}}$, where n_{el} is the number of elements. Let Γ^e denote the boundary of Ω^e. We assume

$$\bar{\Omega} = \bigcup_{e=1}^{n_{\text{el}}} \bar{\Omega}^e , \tag{3.1}$$

$$\emptyset = \bigcap_{e=1}^{n_{\text{el}}} \Omega^e . \tag{3.2}$$

The interior boundary is defined as

$$\Gamma_{\text{int}} = \bigcup_{e=1}^{n_{\text{el}}} \Gamma^e - \Gamma . \tag{3.3}$$

Let V^i and S^i denote the finite-dimensional subsets of $H^1(\Omega)$ satisfying the following conditions:

$$w^i \in V^i \Rightarrow w^i(\boldsymbol{x}) \doteq 0 \quad \forall \boldsymbol{x} \in \Gamma_{g^i} , \tag{3.4}$$

$$\phi^i \in S^i \Rightarrow \phi^i(\boldsymbol{x}) \doteq g^i \quad \forall \boldsymbol{x} \in \Gamma_{g^i} . \tag{3.5}$$

In this paper we assume that both subsets consists of the typical C^0 finite element interpolation functions.

The discrete variational form of the problem is given as follows. Find $\phi^i \in S^i$ such that for all $w^i \in V^i$

$$\begin{aligned} &\int_\Omega \{w^i \boldsymbol{u} \cdot \nabla \phi^i + \nabla w^i \cdot (\boldsymbol{\kappa}^i \cdot \nabla \phi^i) + w^i B^i \phi^2\} \, \mathrm{d}\Omega \\ &+ \sum_{e=1}^{n_{\text{el}}} \int_{\Omega^e} P^i \{\boldsymbol{u} \cdot \nabla \phi^i - \nabla \cdot (\boldsymbol{\kappa}^i \cdot \nabla \phi^i) + B^i \phi^2\} \, \mathrm{d}\Omega \\ &= \int_{\Gamma_{h^i}} w^i h^i \, \mathrm{d}\Gamma , \quad i = 1, \ldots, n_{\text{dof}} , \end{aligned} \tag{3.6}$$

where P^i is a C^{-1} perturbation to the weighting function w^i. The Euler–Lagrange equations corresponding to (3.6) may be obtained by integration-by-parts:

$$\sum_{e=1}^{n_{\text{el}}} \int_{\Omega^e} \tilde{w}^i \{ \boldsymbol{u} \cdot \nabla \varphi^i - \nabla \cdot (\boldsymbol{\kappa}^i \cdot \nabla \phi^i) + B^i \phi^2 \} \, \mathrm{d}\Omega$$

$$+ \int_{\Gamma_{\text{int}}} w^i [\boldsymbol{n} \cdot \boldsymbol{\kappa}^i \cdot \nabla \phi^i] \, \mathrm{d}\Gamma + \int_{\Gamma_{h^i}} w^i \{ \boldsymbol{n} \cdot \boldsymbol{\kappa}^i \cdot \nabla \phi^i - h^i \} \, \mathrm{d}\Gamma = 0 \,, \quad i = 1, \ldots, n_{\text{dof}} \,, \tag{3.7}$$

where [ ] is the "jump" operator.

Remarks

(1) Note that if $P^i = 0$, we have a (Bubnov–) *Galerkin* formulation; if $P^i \neq 0$, we have a *Petrov–Galerkin* formulation. The modified weighting function, that is

$$\tilde{w}^i = w^i + P^i \,,$$

acts only in the element interiors and therefore is allowed to be discontinuous across element boundaries.

(2) Various formulations for P^i, within the framework of streamline-upwind/Petrov–Galerkin (SUPG), sigma weighting, and transport weighting have been tested in [7, 8, 15].

(3) The recent "discontinuity-capturing term" approach of Hughes et al. [9] adds another component to w^i, which results in a smooth but crisp representation of internal and boundary layers.

(4) Brooks and Hughes [1] have shown that for rectangular elements the perturbation term does not affect the weighting of the diffusion term, and for reasonable element shapes the contribution is expected to be negligible.

The spatial discretization of (3.6) leads to a set of nonlinear algebraic equations:

$$\boldsymbol{N}(\boldsymbol{d}) = \boldsymbol{F} \,, \tag{3.8}$$

where $\boldsymbol{d}$ is the vector of (unknown) nodal values of $\boldsymbol{\phi}$, $\boldsymbol{N}$ is the left-hand-side nonlinear vector function of $\boldsymbol{d}$, and $\boldsymbol{F}$ is the right-hand-side constant vector. An incremental load Newton–Raphson iteration scheme is used to solve (3.8).

We employ the following expression for the weighting function associated with the element node a, degree of freedom i:

$$\tilde{N}_a^i = N_a + \xi^i P_a + \eta^i Q_a^i \,, \tag{3.9}$$

where N_a is the isoparametric interpolation function leading to a Galerkin formulation.

The term $\xi^i P_a$ is essentially an SUPG perturbation term similar to the one used in [1]. For isotropic diffusivity tensors, $\boldsymbol{\kappa}^i = \kappa^i \boldsymbol{I}$, where $\boldsymbol{I}$ is the identity tensor, we select P_a and ξ^i as follows:

$$P_a = \tfrac{1}{2} h \boldsymbol{s} \cdot \nabla N_a \,, \tag{3.10}$$

$$\xi^i = \begin{cases} \frac{1}{3}\alpha^i, & \alpha^i \leq 3, \\ 1, & \alpha^i > 3 \end{cases} \tag{3.11}$$

(doubly asymptotic approximation [1]),

where

$$\boldsymbol{s} = \boldsymbol{u}/\|\boldsymbol{u}\|, \tag{3.12}$$

$$h = 2\left(\sum_a |\boldsymbol{s}\cdot\nabla N_a|\right)^{-1} \tag{3.13}$$

("element length"),

$$\alpha^i = \tfrac{1}{2}\|\boldsymbol{u}\|h/\kappa^i \tag{3.14}$$

(element Peclet number).

Discontinuity capturing

To preclude overshooting and undershooting about sharp internal and boundary layers we add a second perturbation term $\eta^i Q_a^i$ to the weighting function. This term, which is similar to the discontinuity-capturing term used in [9], is a function of the local velocity, the solution gradient, and the spatial discretization. The selection procedure for Q_a^i and η^i is described below:

$$\boldsymbol{g}^i = \nabla\phi^i/\|\nabla\phi^i\| \tag{3.15}$$

(solution gradient unit vector),

$$u_{g^i} = \boldsymbol{u}\cdot\boldsymbol{g}^i \tag{3.16}$$

(velocity component parallel to the solution gradient),

$$\boldsymbol{u}_{g^i} = u_{g^i}\boldsymbol{g}^i = (\boldsymbol{u}\cdot\boldsymbol{g}^i)\boldsymbol{g}^i, \tag{3.17}$$

$$h_{g^i} = 2\left(\sum_a |\boldsymbol{g}^i\cdot\nabla N_a|\right)^{-1} \tag{3.18}$$

("element length" in the direction of the solution gradient),

$$\eta^i = \eta(\|\boldsymbol{u}_{g^i}\|/\|\boldsymbol{u}\|) = 2(1 - \|\boldsymbol{u}_{g^i}\|/\|\boldsymbol{u}\|)(\|\boldsymbol{u}_{g^i}\|/\|\boldsymbol{u}\|) \tag{3.19}$$

(parabolic coefficient),

$$Q_a^i = \tfrac{1}{2}h_{g^i}\,\mathrm{sgn}(u_{g^i})\boldsymbol{g}^i\cdot\nabla N_a. \tag{3.20}$$

In the sequel, this scheme will be referred to as EC1.

Remarks

(1) Note that $\eta(\|\boldsymbol{u}_g\|/\|\boldsymbol{u}\|)$ vanishes at the end points of its domain; this is because we

require the discontinuity-capturing contribution to the weighting function to become zero whenever the velocity and the solution gradient vectors are either perpendicular or parallel. The latter condition assures that the SUPG effect is not doubled when the velocity and the gradient vectors are parallel.

(2) For pure convection problems, under the assumption $h_g = h$, we observe that the DC1 and DC2 discontinuity-capturing schemes of Hughes et al. [9] can be obtained by selecting η as 1 and $(1 - \|\boldsymbol{u}_g\| / \|\boldsymbol{u}\|)$, respectively. (For $a \times a$ square elements, the element length selection criterion described in [9] gives $h_g = h = a$ when the $\|\cdot\|_2$ norm is used.) In this case, for $\|\boldsymbol{u}_g\| / \|\boldsymbol{u}\| = \frac{1}{2}$, our EC1 scheme leads to the same discrete equations as the DC2 scheme does.

(3) For the EC1 scheme described above (and for the DC1 and DC2 schemes given in [9]) the discontinuity-capturing contribution to the weighting function depends only on the unit vector $\boldsymbol{g}$. Therefore, even a very small but nonzero gradient in a solution, which can be called smooth, leads to the same level of contribution as a very sharp gradient. This concern becomes especially legitimate when one considers the effect of the discontinuity-capturing component of the weighting function on the nonconvective terms of the differential equation system. In our alternate formulation, we require that the discontinuity-capturing component be dependent on not only the direction but also the magnitude of the solution gradient vector. This is achieved by replacing the unit vector $\boldsymbol{g}^i$ in the definition of Q_a^i by the vector $\boldsymbol{G}^i$ which incorporates this magnitude as follows:

$$Q_a^i = \tfrac{1}{2} h_{g^i} \operatorname{sgn}(u_{g^i}) \boldsymbol{G}^i \cdot \nabla N_a \,, \tag{3.21}$$

$$\boldsymbol{G}^i = h_{g^i} (\|\nabla \phi^i\| / \phi_0^i) \boldsymbol{g}^i \,, \tag{3.22}$$

where ϕ_0^i is a global scaling value for ϕ^i. This scheme will be referred to as EC2.

(4) For even linear problems the EC1 and EC2 schemes also lead to nonlinear discrete equations due to the dependence of the weighting function on the solution.

4. Reaction-dominated problems

For convection-reaction problems, as the flow velocity at a point in the flow field assumes or approaches the value zero, the problem locally becomes reaction-dominated. Therefore, in the presence of sharp gradients in the solution due to high reaction rates, one may encounter spurious oscillations in the numerical solution. Similar numerical difficulties may be observed in diffusion-reaction problems as the diffusion rate becomes too low. In our effort to cure such complications, we perform a one-dimensional analysis of the numerical schemes used. This analysis is described in the sequel.

Consider the following linear convection-reaction equation with constant velocity u and reaction rate B:

$$B\phi + u\phi_{,x} = 0 \,. \tag{4.1}$$

The exact solution of this problem takes the form:

$$\phi = e^{-Bx/u} . \tag{4.2}$$

Assuming a discretization with constant element length h, the coordinate and the exact solution at a mesh point j can be written as follows:

$$x_j = hj , \tag{4.3}$$

$$\phi_j = e^{-2\gamma j} , \tag{4.4}$$

where

$$\gamma = \tfrac{1}{2}hB/u . \tag{4.5}$$

Finite element discretization of (4.1) leads to the following equation for the jth node:

$$\{\gamma^* \boldsymbol{D}_r + \boldsymbol{D}_1 + \delta^* \boldsymbol{D}_2\} \begin{pmatrix} \phi_{j-1} \\ \phi_j \\ \phi_{j+1} \end{pmatrix} = 0 , \tag{4.6}$$

where

$$\gamma^* = \tfrac{1}{2}h(B + \tilde{B})/(u + \tilde{u}) , \tag{4.7}$$

$$\delta^* = 2\tilde{\kappa}/(h(u + \tilde{u})) . \tag{4.8}$$

Here $\tilde{B}$, $\tilde{u}$, and $\tilde{\kappa}$ are the numerical contributions to the reaction rate, the convection velocity, and the diffusivity, respectively. The stencils $\boldsymbol{D}_r$, $\boldsymbol{D}_1$, and $\boldsymbol{D}_2$ are defined as follows:

$$\boldsymbol{D}_r = (2r, 2(1-2r), 2r) , \tag{4.9}$$

$$\boldsymbol{D}_1 = (-\tfrac{1}{2}, 0, \tfrac{1}{2}) , \tag{4.10}$$

$$\boldsymbol{D}_2 = (-\tfrac{1}{2}, 1, -\tfrac{1}{2}) . \tag{4.11}$$

The parameter r in (4.9) is determined by the integration rule used for the element coefficient matrix corresponding to the reaction term. The most common choices for r are given in Table 1.

We need to investigate the conditions under which (4.6) admits the exact solution (4.4). Satisfaction of these conditions leads to nodally exact finite element solutions. Substitution of (4.4) into (4.6) results in the following equation:

$$\{\gamma^* \boldsymbol{D}_r + \boldsymbol{D}_1 + \delta^* \boldsymbol{D}_2\} \boldsymbol{E} = 0 , \tag{4.12}$$

where the stencil $\boldsymbol{E}$ is defined as:

$$\boldsymbol{E} = (e^{-2\gamma}, 1, e^{2\gamma}) . \tag{4.13}$$

Table 1

r	rule
$\frac{1}{4}$	1-point Gaussian quadrature
$\frac{1}{6}$	2-point Gaussian quadrature (exact integration)
0	trapezoidal

With some algebraic manipulation, from (4.12) we obtain:

$$\delta^* = -\coth\gamma + \gamma^*(1/\sinh^2\gamma + 4r)\,. \tag{4.14}$$

Assuming that no numerical contribution to the reaction rate or the convection velocity is introduced (i.e. $\tilde{B}=0$, $\tilde{u}=0$), we get an expression for the numerical contribution to the diffusion term which leads to nodally exact solutions. That is,

$$\tilde{\kappa} = \tilde{\kappa}(\gamma) = \tfrac{1}{2}uh\{-\coth\gamma + \gamma(1/\sinh^2\gamma + 4r)\}\,. \tag{4.15}$$

This expression for $\tilde{\kappa}$ is used to add a diffusion term for reaction-dominated problems. We will call this the DRD term.

We generalize this concept to multi dimensions by defining a numerical diffusivity tensor as follows:

$$\tilde{\boldsymbol{\kappa}} = \tilde{\kappa}(\gamma)\boldsymbol{ss} + \tilde{\kappa}(\infty)(\boldsymbol{tt} + \boldsymbol{vv})\,, \tag{4.16}$$

where

$$\gamma = \tfrac{1}{2}hB/\|\boldsymbol{u}\|\,, \tag{4.17}$$

while s and h are given by (3.12) and (3.13). The unit vectors $\boldsymbol{t}$ and $\boldsymbol{v}$ are orthogonal to $\boldsymbol{s}$ and each other. Note that for a purely one-dimensional problem, since only the gradient in the s-direction is nonzero, there will be no contribution due to the $\boldsymbol{tt}$ and $\boldsymbol{vv}$ terms. Similarly, for a two-dimensional problem, if we choose $\boldsymbol{v}$ to be orthogonal to our two-dimensional space, then there will be no contribution due to the $\boldsymbol{vv}$ term.

Note that as $\tilde{B}\to 0$, $\gamma\to 0$ and $\tilde{\kappa}\to 0$, while as $\tilde{u}\to 0$, $\gamma\to\infty$ and $\tilde{\kappa}\to 4rB(\frac{1}{2}h)^2$. A similar analysis is presented in Appendix A for the one-dimensional linear diffusion-reaction equation.

We now search for a Petrov–Galerkin method which produces the same effect for the one-dimensional problems. Select a weighting function of the form

$$\tilde{w} = w + \tfrac{1}{2}\beta h w_{,x}\,, \tag{4.18}$$

where β is the parameter to be determined resulting in nodally exact solutions. Finite element discretization of (4.1) with the weighting function defined as above leads again to (4.12) with γ^* and δ^* given as:

$$\gamma^* = \gamma/(1-\beta\gamma)\,, \tag{4.19}$$

$$\delta^* = \beta/(1-\beta\gamma)\,. \tag{4.20}$$

Note that, in this case, $\tilde{B}=0$ but

$$\tilde{u} = -\tfrac{1}{2}\beta hB \tag{4.21}$$

and

$$\tilde{\kappa} = \tfrac{1}{2}\beta hu\,. \tag{4.22}$$

From (4.14), (4.19), and (4.20) we obtain an expression for β which produces nodally exact solutions. That is

$$\beta = \beta(\gamma) = \{-\coth \gamma + \gamma(1/\sinh^2 \gamma + 4r)\}/(1 - \gamma \coth \gamma)\,. \tag{4.23}$$

Note that as $B \to 0$, $\gamma \to 0$ and $\beta \to 0$, while as $u \to 0$, $\gamma \to \infty$ and $\beta \to 4r$.

5. Numerical examples

All examples were run in double precision on a VAX 8600 with 32-bit single-precision word. We tested and compared the following methods: For convection-dominated problems:

(a) streamline-upwind/Petrov–Galerkin (SUPG);
(b) SUPG with discontinuity-capturing type 1 (SUPG + EC1) (see Section 3);
(c) SUPG with discontinuity-capturing type 2 (SUPG + EC2) (see Section 3).

For convection-reaction problems:

(a) SUPG;
(b) SUPG with diffusion for reaction-dominated regions (SUPG + DRD) (see Section 4).

5.1. Convection of a single component in a flow field skew to the mesh with downwind essential boundary condition

This problem is governed by a linear differential equation, which can be obtained as a special case of any one of the equations (2.1)–(2.3) by nullifying the source (reaction) term. Furthermore, the physical diffusion is negligibly small, therefore the transport problem is convection dominated. We used a 20 by 20 square finite element mesh. The inflow boundary conditions involve a discontinuity resulting in an internal discontinuity skew to the mesh. The outflow boundary conditions, due to the convection-dominated nature of the problem, result in sharp boundary layers which can essentially be viewed as discontinuities. Because of the discontinuities, these types of problems, which were first considered by Hughes and Brooks [11], constitute a difficult test for the soundness of a method.

The flow fields considered are given as $u_2/u_1 = 2$ (Fig. 1), $u_2/u_1 = 1$ (Fig. 2), and $u_2/u_1 = \frac{1}{2}$ (Fig. 3). The numerical solutions are compared to the nodally exact solutions. The results for the Galerkin formulation (not shown) are highly oscillatory. Figure 1 ($u_2/u_1 = 2$) shows significant improvements in the solutions obtained by the EC1 and EC2 schemes compared to the SUPG scheme. The EC1 and EC2 solutions do not exhibit the strong overshoots of the SUPG solution at the downwind boundary. Though not as significant, some improvements are observed also at the internal discontinuity. Figure 2 ($u_2/u_1 = 1$) shows improvements at the internal and boundary layer discontinuities. Slight smearing is observed at the downwind boundary layer. Figure 3 ($u_2/u_1 = \frac{1}{2}$) shows improvements at the internal discontinuity with little smearing at the downwind boundary layer.

Remark

In our EC2 scheme, for this set of problems, we used a scaling parameter of 1 (i.e., $\phi_0 = \phi_{\max} - \phi_{\min} = 1$). In all three cases, the EC1 and EC2 terms are expected to have a

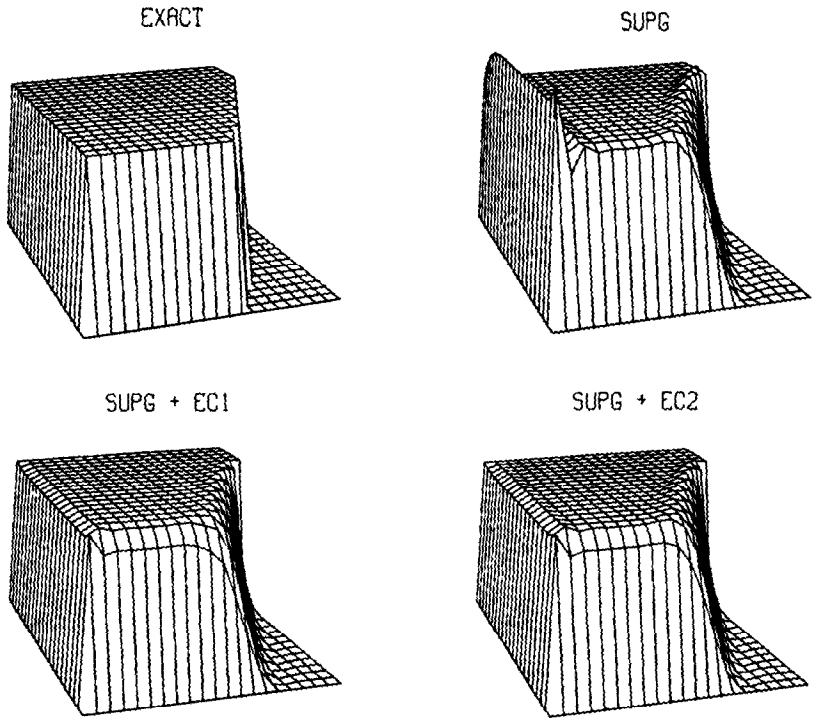

Fig. 1. Convection of a single component in a flow field skew to the mesh: $u_2/u_1 = 2$.

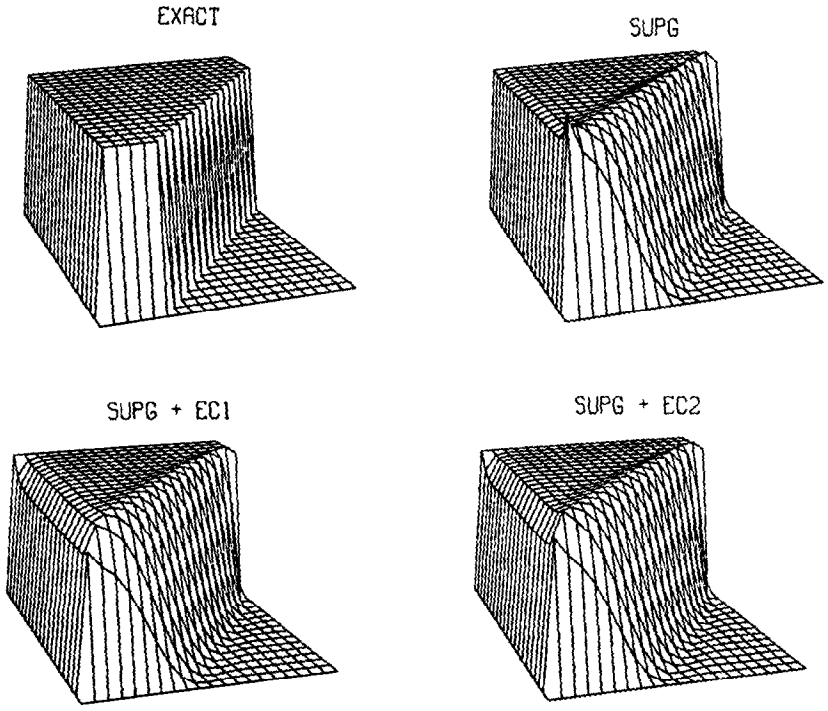

Fig. 2. Convection of a single component in a flow field skew to the mesh: $u_2/u_1 = 1$.

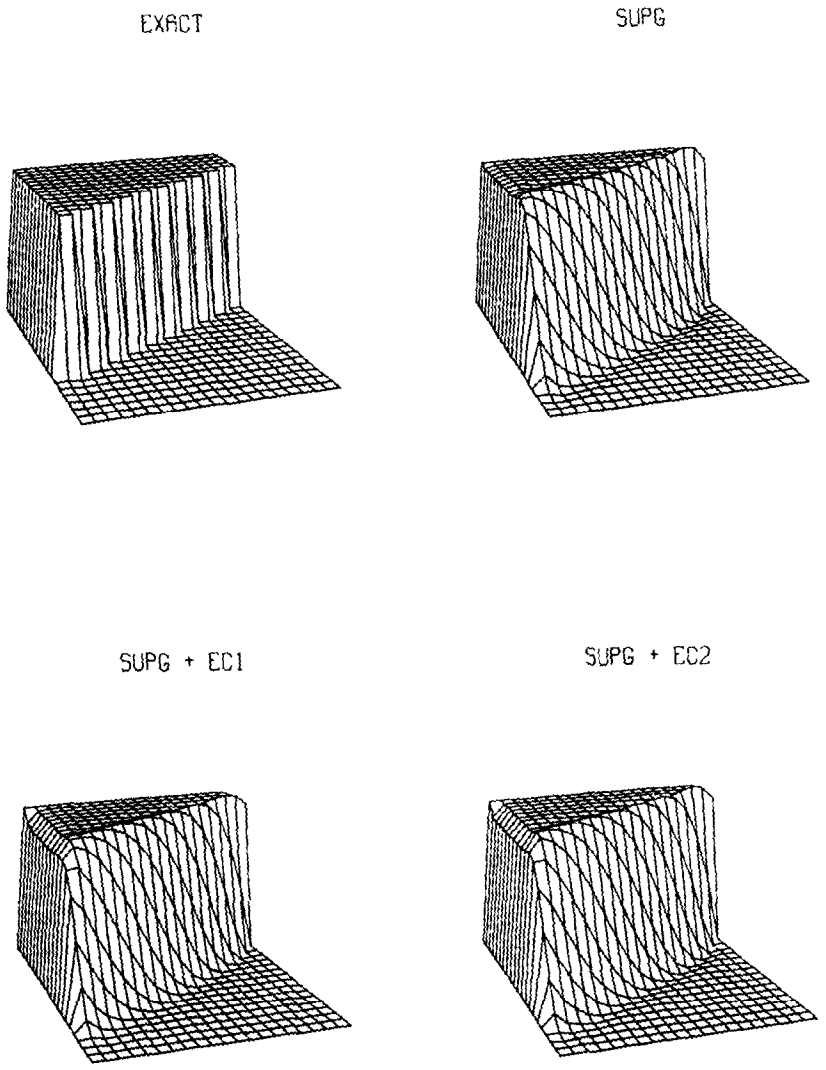

Fig. 3. Convection of a single component in a flow field skew to the mesh: $u_2/u_1 = \frac{1}{5}$.

significant effect only at the sharp boundary layers. Across the elements where these boundary layers are located, in a direction normal to the discontinuity, we have a unit jump ($\phi_{max} - \phi_{min} = 1$) in the solution. Therefore, it is normal that the EC1 and EC2 schemes result in very similar solutions.

5.2. *Convection of a single component in a rotating flow field* ("*Donut Problem*")

The differential equation which governs this problem is the same as the one governing the set of problems of Section 5.1. The physical diffusivity is again negligible. The rotational flow field has an axis of rotation passing through the center of the square domain. This convection-dominated problem, which was first considered in [11], is used as a test of accuracy in terms of the amplitude decay due to numerical diffusion.

We employed a 30 by 30 mesh. Figure 4 shows that the solutions obtained by the SUPG,

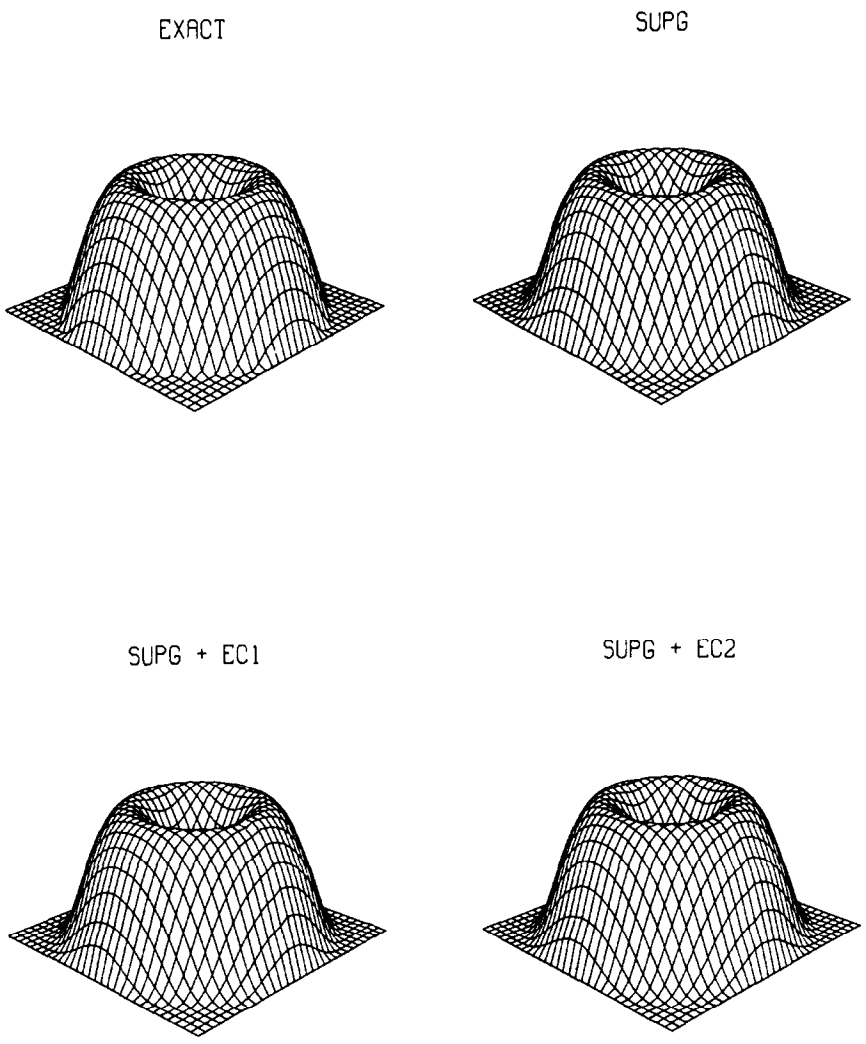

Fig. 4. Convection of a single component in a rotating flow field.

EC1, and EC2 schemes are all almost identical to the exact solution with nearly no amplitude decay. For this problem, classical upwind differences result in a 70 percent amplitude decay due to excessive crosswind diffusion [8].

Remark

In this problem the velocity vector is perpendicular (nearly perpendicular in a discrete sense) to the gradient in the solution. As $\|\boldsymbol{u}_g\|/\|\boldsymbol{u}\|$ approaches zero, because of (3.19), the EC contribution to the weighting function vanishes. This is why the SUPG, EC1, and EC2 schemes produce almost identical solutions. In fact, as $\|\boldsymbol{u}_g\|/\|\boldsymbol{u}\| \to 0$,

$$\eta = \mathrm{O}(\|\boldsymbol{u}_g\|/\|\boldsymbol{u}\|) \tag{5.1}$$

and

$$\eta Q_a \boldsymbol{u} \cdot \nabla \phi = \mathrm{O}((\|\boldsymbol{u}_g\|/\|\boldsymbol{u}\|)^2)\,. \tag{5.2}$$

5.3. Convection-reaction problems

For these problems, we neglect the diffusion terms in (2.4). From (2.4) we can write an equation relating C^B to C^A, that is

$$C^A + (1/b)C^B = \text{constant}\,. \tag{5.3}$$

Therefore one needs to solve only one of the equations for the concentrations. The velocity is assumed to have a parabolic profile as follows:

$$u_1 = u_1(x_2) = u_{\max}(1 - x_2^2)\,. \tag{5.4}$$

Figure 5(a) shows the 40 by 20 rectangular nonuniform finite element mesh used for these problems. We tested our formulations on the following two specific problems.

5.3.1. Linear convection reaction for a single-component system

For this case we neglect the heat of reaction ΔH and assume isothermal conditions. Even though in this linear problem we have two components, we need to solve only one convection-reaction equation for a single component. The boundary conditions for this single component are given in Fig. 5(b). The data for this problem are given in Table 2. The exact solution has the form:

$$C_A = C_0^A \exp(-B^2 x_1/u_1)\,, \tag{5.5}$$

where C_0^A is the Dirichlet boundary condition at $x_1 = 0$ and B^2 is given by (2.6). Figure 6 shows the exact, SUPG, and SUPG + DRD solutions for the component C^A. The SUPG solution exhibits a 57 percent undershoot while the DRD scheme provides a significant improvement by resulting in only a 12 percent undershoot.

5.3.2. Nonlinear convection reaction for a two-component system

In this problem no assumptions regarding the heat of reaction or the temperature profile were made. The data given in Table 2 were selected based on realistic chemically reacting systems [14]. The boundary conditions are shown in Fig. 5(c). The "exact" solution is obtained by a forward difference scheme starting from the Dirichlet-type boundary condition at $x_1 = 0$. We used the following equation to obtain the "exact" solution:

Table 2
Data used for the linear and nonlinear problems.

	Linear	Nonlinear
k_0	5.0	3.0×10^8
$\Delta H/(\rho c_p)$	0.0	−100
E/R	0.0	10000
$u_{\max}$	1.0	1.0

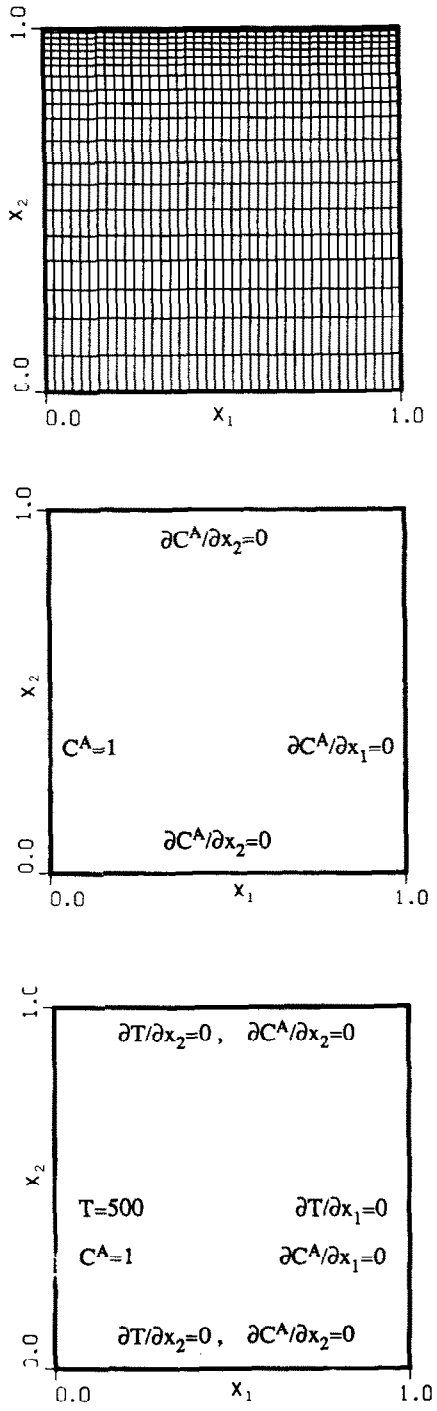

Fig. 5. Finite element mesh and boundary conditions for the convection-reaction problems. (a) Finite element mesh. (b) Boundary conditions for the single-component problem. (c) Boundary conditions for the two-component problem.

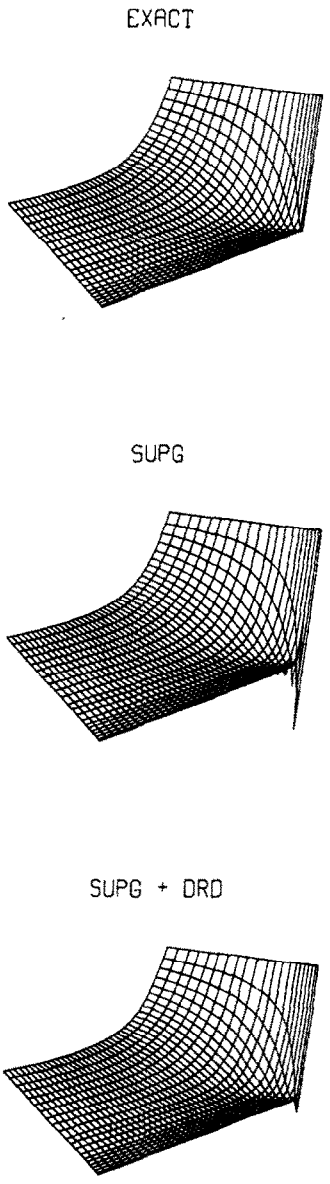

Fig. 6. Linear convection reaction for a single-component system.

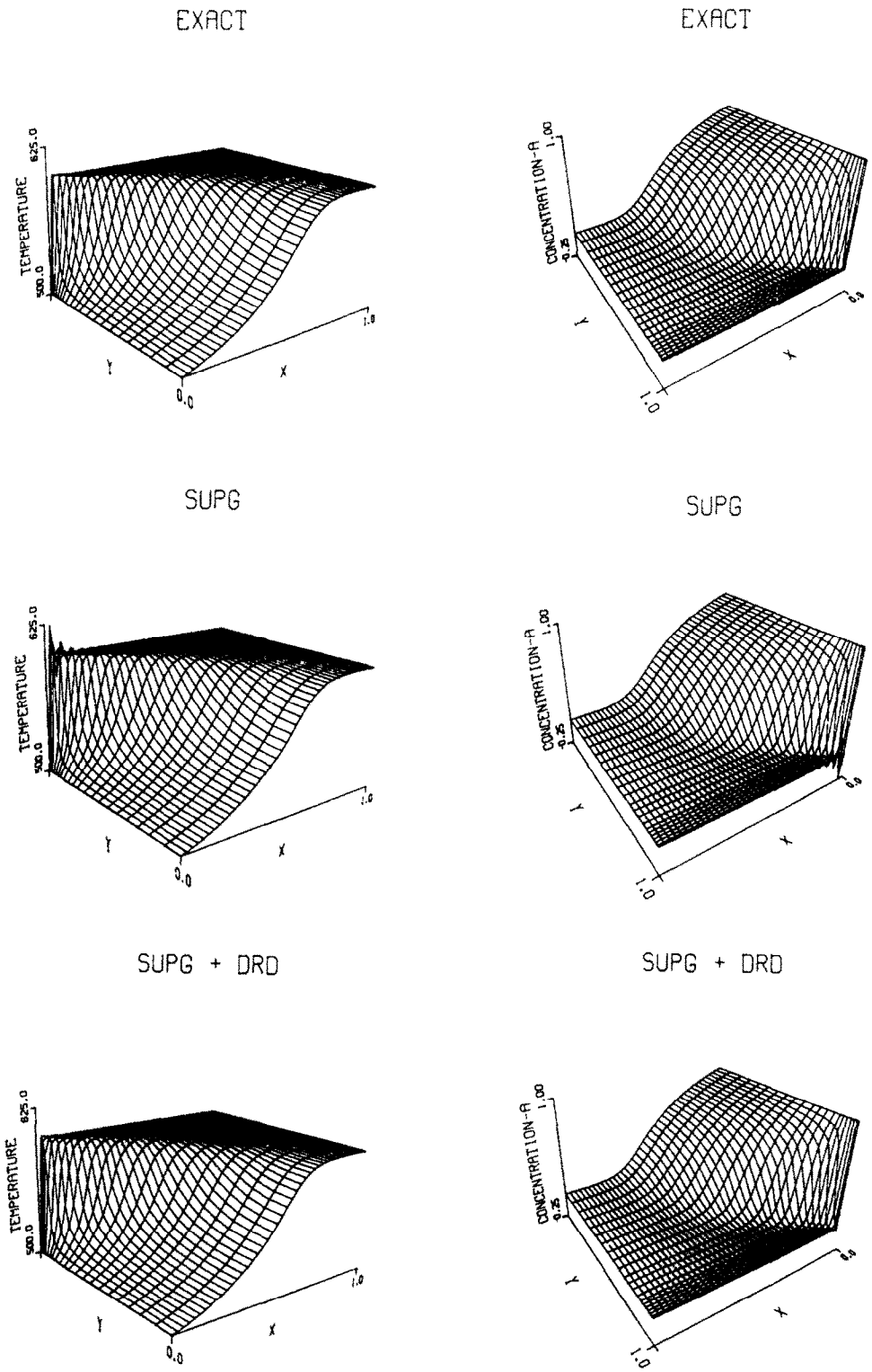

Fig. 7. Nonlinear convection reaction for a two-component system.

$$\phi_{j+1}^{i} = \phi_{j}^{i} - \Delta x_1 (B^i \phi^2 / u_1)_j \,, \quad i = 1, \ldots, n_{\text{dof}} \,, \tag{5.6}$$

where B^i is given by (2.6). The step size (Δx_1) was decreased until the accuracy of the solution was not affected. Figure 7 shows the exact, SUPG, and SUPG + DRD solutions for T and C^A. Where the problem becomes reaction-dominated, the SUPG scheme produces 24 percent undershoot and overshoot for the concentration of the component A and the temperature, respectively. The DRD scheme shows a significant improvement with less than 2 percent undershoot and overshoot.

6. Conclusions

In this paper we have presented formulations which complement the streamline-upwind/Petrov–Galerkin schemes for convection-diffusion-reaction systems. The SUPG formulation in some cases exhibits oscillations about internal and boundary layer discontinuities. Such discontinuities may be observed for convection-dominated and reaction-dominated problems. To minimize such oscillations for convection-dominated flows, we proposed the addition of a "discontinuity-capturing term" to the weighting function. This term, which acts in the direction of the gradient in the solution, depends on the spatial discretization. It may also depend on the magnitude of the "jump" in the solution across an element in the direction of the gradient.

For reaction-dominated problems, by adding a second-order term to the differential equation we were able to minimize the oscillations about sharp layers. In fact, via a one-dimensional analysis, we can determine the coefficient of this second-order term which leads to nodally exact solutions for the one-dimensional linear problems. The second-order term becomes significant only when the reaction rate is too high. We applied our proposed formulations to various steady-state linear and nonlinear problems. The solutions obtained are accurate with minimal oscillations and minimal numerical dissipation.

Appendix A. Analysis of the finite element discretization for the one-dimensional diffusion-reaction equation

Consider the following linear diffusion-reaction equation with constant diffusion coefficient κ and reaction rate B:

$$B\phi = \kappa \phi_{,xx} \,. \tag{A.1}$$

The exact solution for this equation takes the form:

$$\phi = \mathrm{e}^{\pm x\sqrt{B/\kappa}} \,. \tag{A.2}$$

Assuming a discretization with constant element length h, the coordinate and the exact solution at node j can be written as follows:

$$x_j = hj\,, \tag{A.3}$$

$$\phi_j = \mathrm{e}^{\pm 2\beta j}\,. \tag{A.4}$$

where

$$\beta^2 = (B/\kappa)(\tfrac{1}{2}h)^2\,. \tag{A.5}$$

Following a procedure similar to the one in Section 4, we obtain:

$$\{(\beta^*)^2 \boldsymbol{D}_r + \boldsymbol{D}_2\}\boldsymbol{E} = 0\,, \tag{A.6}$$

where

$$(\beta^*)^2 = (\tfrac{1}{2}h)^2(B + \tilde{B})/(\kappa + \tilde{\kappa})\,. \tag{A.7}$$

Algebraic manipulation of (A.6) leads to

$$1/(\beta^*)^2 = 4r + 1/\sinh^2\beta\,. \tag{A.8}$$

Assuming that no numerical reaction rate is introduced (i.e. $\tilde{B} = 0$), we get an expression for the numerical diffusion term which leads to nodally exact solutions:

$$\tilde{\kappa}/\kappa = 4r\beta^2 + \beta^2/\sinh^2\beta - 1\,. \tag{A.9}$$

Alternately we can have

$$\tilde{\kappa}/B(2/h)^2 = 4r + 1/\sinh^2\beta - 1/\beta^2\,. \tag{A.10}$$

Note that as $B \to 0$, $\beta \to 0$ and $\tilde{\kappa} \to 0$, while as $\kappa \to 0$, $\beta \to \infty$ and $\tilde{\kappa} \to 4rB(\tfrac{1}{2}h)^2$.

References

[1] A.N. Brooks and T.J.R. Hughes, Streamline upwind/Petrov–Galerkin formulations for convection dominated flows with particular emphasis on the incompressible Navier–Stokes equations, Comput. Meths. Appl. Mech. Engrg. 32 (1982) 199–259.

[2] H.A. Deans and L. Lapidus, A computational model for predicting and correlating the behavior of fixed bed reactors: I. Derivation of model for nonreactive systems, AIChEJ. (1960) 656–663.

[3] H.A. Deans and L. Lapidus, A computational model for predicting and correlating the behavior of fixed-bed reactors: II. Extension to chemically reactive systems, AIChEJ. (1960) 663–668.

[4] B.A. Finlayson, Packed bed reactor analysis by orthogonal collection, Chem. Engrg. Sci. 26 (1971) 1082–1091.

[5] G.F. Fromont and K.B. Bischoff, Chemical Reactor Analysis and Design (Wiley, New York, 1979).

[6] R.F. Heinemann and A.B. Poore, Multiplicity, stability, and oscillatory dynamics of the tubular reactor, Chem. Engrg. Sci. 36 (1981) 1411–1419.

[7] T.J.R. Hughes and A.N. Brooks, A theoretical framework for Petrov–Galerkin methods with discontinuous weighting functions: Application to the streamline upwind procedure, in: R.H. Gallagher, eds. D.N. Norrie, J.T. Oden and O.C. Zienkiewicz, Finite Elements in Fluids (Wiley, London, 1982) 46–65.

[8] T.J.R. Hughes, M. Mallet, Y. Taki, T. Tezduyar and R. Zanutta, A one-dimensional shock capturing finite element method and multi-dimensional generalizations, in: F. Angrand, A. Dervieux, J.A. Desideri and R. Glowinski, eds., Numerical Methods for the Euler Equations of Fluid Dynamics (SIAM, Philadelphia, PA, 1985) 371–408.

[9] T.J.R. Hughes, M. Mallet and A. Mizukami, A new finite element formulation for computational fluid dynamics: II. Beyond SUPG, Comput. Meths. Appl. Mech. Engrg. 54 (1986) 341–355.
[10] T.J.R. Hughes, M. Mallet and L. Franca, New finite element methods for the compressible Euler equations, in: R. Glowinski and J.L. Lions, eds., Computing Methods in Applied Sciences and Engineerings VII (North-Holland, Amsterdam, 1986).
[11] T.J.R. Hughes and A. Brooks, A multidimensional upwind scheme with no crosswind diffusion, in: T.J.R. Hughes, ed., Finite Element Methods for Convection Dominated Flows (ASME, New York, 1979) 19–35.
[12] K.F. Jensen and W.H. Ray, The bifurcation behavior of tubular reactors, Chem. Engrg. Sci. 37 (2) (1982) 199–222.
[13] R. Mihail and C. Iordache, Performances of some numerical techniques used for simulation of fixed bed catalystic reactors, Chem. Engrg. Sci. 31 (1976) 83–86.
[14] V. Pinjala, Wrong-way behavior in fixed-bed catalystic reactors: Pseudo-homogeneous dispersion model, Ph.D. Thesis, Chemical Engineering Department, University of Houston, Houston, TX, 1985.
[15] T.E. Tezduyar and T.J.R. Hughes, Finite element formulations for convection dominated flows with particular emphasis on the compressible Euler equations in: Proceedings AIAA 21st Aerospace Sciences Meeting, AIAA Paper 83-0125, Reno, NV, 1983.